ARTICLE

Interplay of Sequence, Conformation, and Binding at the Peptide−Titania Interface as Mediated by Water

Adam A. Skelton, Taining Liang, and Tiffany R. Walsh*

Department of Chemistry and Centre for Scientific Computing, University of Warwick, Coventry CV4 7AL, U.K.

ABSTRACT The initial stages of the adsorption of a hexapeptide at the aqueous titania interface are modeled using atomistic molecular dynamics simulations. This hexapeptide has been identified by experiment [Sano, K. I.; Shiba, K. *J. Am. Chem. Soc.* **2003**, *125*, 14234] to bind to Ti particles. We explore the current hypothesis presented by these authors that binding at this peptide−titania interface is the result of electrostatic interactions and find that contact with the surface appears to take place via a pair of oppositely charged groups in the peptide. Our data indicate that the peptide may initially recognize the water layers at the interface, not the titania surface itself, via these charged groups. We also report results of simulations for hexapeptide sequences with selected single-point mutations for alanine and compare these behaviors with those suggested from observed binding affinities from existing alanine scan experiments. Our results indicate that factors in addition to electrostatics also contribute, with the structural rigidity conferred by proline suggested to play a significant role. Finally, our findings suggest that intrapeptide interaction may provide mechanisms for surface detachment that could be detrimental to binding at the interface.

KEYWORDS: molecular dynamics • nanotechnology • peptides • surface chemistry • noncovalent interactions

INTRODUCTION

Screening techniques are now routinely used to identify peptide sequences that can recognize synthetic inorganic materials (1−7). The utility of these peptides has been recently demonstrated in "green" materials fabrication (8−17) including procellular coatings (14), nanophotonics constructs (10) and three-dimensional (3D) nanostructures (16). Despite recent advances, the basis of this recognition behavior, in terms of both binding affinity and materials specificity, remains poorly understood. Recent findings suggest this behavior cannot be attributed to residue content alone (18−20); the notion that the sequence of a strong-binding peptide must confer particular structural, dynamic, and thermodynamic characteristics that favor binding appears to be emerging in the literature. A recently identified hexapeptide sequence, RKLPDA, has been conjectured to interact with Ti particles via electrostatic interactions (21). This hypothesis was, in part, supported by alanine scan experiments (21), indicating diminished binding upon point mutation of the charged residues Asp and Arg. Adhesion force analysis experiments (22) also strongly suggested that electrostatic interactions play a critical role at the interface between titania and this hexapeptide. However, additional data point to a more complex picture of the hexapeptide binding at the interface; first, mutation of the neutral Pro residue also reduced affinity, and second, mutation of the charged Lys actually *increased* affinity. This hexapeptide sequence has been successfully deployed in biomaterials applications via conjugation to the bone morphogenic protein (23) and also to proteins containing the cell attachment motif RGD (24).

Data from the structural determination of biomolecules at such biointerfaces are rare (25, 26), although clues may be obtained from solution structures of inorganic-binding peptides (for example, calcium phosphate binders (27)). However, these solution studies may not clearly indicate how the solution structure of the peptide might perturb upon adsorption at the inorganic surface. Indirect information points to conformational influences on peptide-surface binding; e.g., mutations other than those for alanine suggest links between conformation and affinity (28), and similarities/differences in binding to platinum surfaces (29) and gold surfaces (20) between the linear and cyclic forms of the same peptide sequence have also been observed. In our case, the structural features of the hexapeptide−titania interface have not yet been determined. Therefore, this system provides a tractable test case for exploring the interplay between sequence, conformation, and properties (in this case, binding behaviors) that can be feasibly explored using molecular simulation under aqueous conditions.

Although there has been considerable growth in the experimental study of peptide−inorganic recognition, there are not as many modeling studies in this area. It is essential to understand the nature of molecular recognition and, ultimately, the degree of affinity of a selected peptide to a given surface, so that this behavior can be rationalized, predicted, and optimized for a range of applications (30); molecular dynamics (MD) simulation can serve as a complementary tool alongside other experimental characterization techniques in realizing this goal. A number of modeling studies have appeared for peptide−metal recognition, in-

* E-mail: t.walsh@warwick.ac.uk.
Received for review March 13, 2009 and accepted May 18, 2009
DOI: 10.1021/am9001666

Published on Web 06/10/2009

cluding gold (20, 31) and platinum (32, 33). In particular, modeling studies of phage-display peptides with different levels of affinity to the Pt(100) surface (32) showed good agreement with experimental data despite using only van der Waals (vdw) terms to describe the nonbonded interactions. Peptide–oxide surface MD simulations have been reported for peptides selected to bind to copper oxide and zinc oxide surfaces (34). Simulations of the peptide–nanotube interface (35) have been reported that support trends that were observed experimentally (36), in terms of the relative binding affinity. While not immediately applicable to the recognition phenomena demonstrated by selected peptides, simulation studies of dipeptides (37) and collagen fragments (38) interacting with the rutile titania surface have also been reported. The former study focused on the direct interaction of carboxylate groups with the undercoordinated Ti atoms present on the surface.

So far, the role of the solvent has not been widely considered in the process of peptide binding at the interface, although a few simulation studies have recently appeared where calculated free-energy profiles for amino acid (or analogues) adsorption at aqueous interfaces (39–41) have been presented. In this work, we investigate the role played by structured water at the hydrophilic titania surface in peptide–inorganic recognition. Similar to what has been demonstrated experimentally for peptide–DNA binding (42), our simulation data presented herein indicate that the initial stages of recognition could proceed via peptide binding to structured water at the interface rather than through recognition of the inorganic surface itself. In this work, we explore the initial stages of adsorption of the hexapeptide RKLPDA onto the rutile TiO_2 (110) surface under aqueous conditions. Our aims of this study are the following: to use this relatively small system to investigate the importance of the charged groups in binding at the interface in order to test the hypothesis of electrostatically-driven binding, to explore the influence on peptide binding of the well-known phenomenon of water structuring at the TiO_2–water interface, and to examine the electrostatic and conformational effects on the interfacial binding stability for a selected number of alanine point mutations of the hexapeptide.

METHODS

We performed atomistic MD simulations of a single hexapeptide molecule, RKLPDA, adsorbed onto the rutile TiO_2 (110) surface. The hexapeptide in our simulations was modeled at neutral pH, with conventional assignment of protonation states, with Arg and Lys carrying a positive charge and Asp carrying a negative charge. There is a good deal of evidence to support our choice of the surface model. First, it is well-known that upon exposure to air, Ti metal forms a thick oxide layer with approximate TiO_2 stoichiometry (43, 44). Further, the adsorption behavior from solution onto TiO_2 surfaces was found to be similar for both amorphous and crystalline titania films (45) for noncovalently attached species. The spectroscopic studies of McQuillan and co-workers suggest that both Lys (45) and Asp (46) are not covalently attached to titania at neutral pH. The rutile (110)–water interface has been extensively characterized by both experiment and theory. Moreover, simulations of the rutile (110)–water interface (47, 48) indicate that the vertical and lateral spatial ordering of the water layers is not significantly different out to and beyond the second water layer (6 Å from the surface), regardless of the hydroxylation or charged state (neutral or negatively charged). Also, trends in orientational ordering within these two layers were not found to be significantly different for all but the fully hydroxylated neutral surface. Therefore, in the case of the first water layer, the difference, say, between the display of two H atoms belonging to the same first-layer water molecule or instead displayed as part of two surface hydroxyl groups, should be not significant for the purposes of our study. Finally, the diffusion coefficients of water as a function of distance from the surface were found to be insensitive to the charged or hydroxylation state (47) of the surface.

Our MD simulations were performed using the DL_POLY package (49). We modeled a five-layer titania slab, presenting the (110) surface with dimensions of roughly 39×37 Å^2. Periodic boundary conditions were used such that the average interslab (vertical) spacing was around 48 Å, amounting to a total of 2123 water molecules located between neighboring slabs. This yielded a central layer of bulk water with an approximate thickness of 25 Å. Counterions were included to ensure an overall charge neutrality of the simulation cell. Long-range electrostatic interactions were handled using Ewald summation, which should be adequate in terms of recovering a reasonable description of atom density profiles (48). The force field used to describe interactions in the system comprised an established potential for describing the titania slab under aqueous conditions (47, 48), the CHARMM27 (50) for describing the peptide, and a modified TIP3P (51) potential for describing water. Simulations were performed in the canonical (*NVT*) ensemble under ambient pressure and temperature conditions, such that the bulk TIP3P water density was recovered in the central water region between the titania slabs. The Nosé–Hoover (52–54) thermostat was used, with the equations of motion integrated with a time step of 1 fs. We equilibrated our system over a total period of 160 ps for each production run. During this equilibration process, we first held the peptide fixed in space in its original conformation, letting all water molecules move for 20 ps. The peptide was then also released, and the system temperature was gradually increased in steps of 50 K from 0 K up to 250 K. The system was equilibrated for 20 ps at each intermediate temperature, before commencing with the production run at 298 K. Production runs were typically of durations in excess of 2 ns. Frames were saved every 0.5 ps in the production runs.

We took particular care in generating initial configurations for all of our runs and followed a variety of approaches in creating initial geometries. Our first approach was to run simulations of the peptide–titania interface using an implicit solvent model (55, 56). From a number of these implicit solvent runs, we identified and extracted the configurations with the greatest binding to the titania surface. We chose the five configurations with the strongest binding, and soaked these configurations in explicit water (thereafter following the equilibration procedure as outlined above). We created additional initial configurations by vertically displacing (in the direction perpendicular to the surface plane) each of these five configurations by both 2 and 3 Å, before again soaking the system in an explicit solvent. Second, we ran a series of simulations where the peptide was initially located in the center of the (explicitly solvated) simulation cell and was slowly dragged onto the surface by application of a weak harmonic tethering potential, acting in the direction perpendicular to the surface plane. We explored the effect of the tether attachment point on the peptide, attaching at either of the backbone chain ends (either Asp C_α or Arg C_α), the chain midpoint (center C_α), or combinations of chain end and midpoint. Finally, we also performed extensive simulations in the isothermal–isobaric (*NPT*) ensemble of the peptide in an explicit solvent, without the pres-

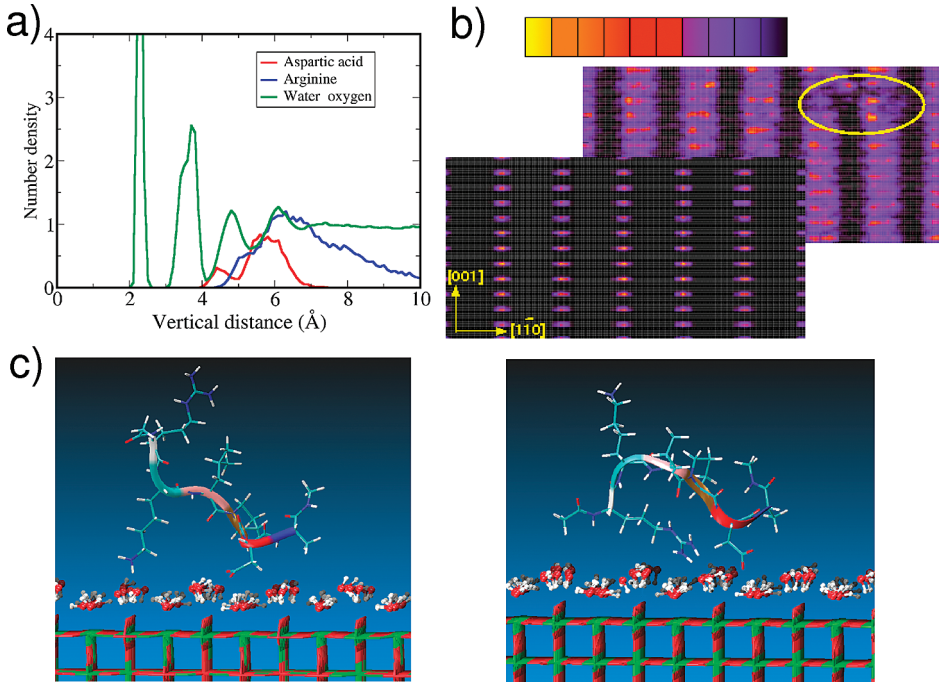

FIGURE 1. (a) Vertical density profiles of water and peptide side groups, as a function of the distance from the titania surface. (b) Lateral density profiles of water layers 1 (front) and 3 (back), with a scale bar (top), with yellow indicating areas of highest density and black indicating areas of lowest density. The yellow ring indicates where Asp has bound to the water. (c) Snapshots of stable, water-bound KD (left) and RD (right) configurations (only the first two water layers are shown for clarity).

ence of the titania surface. In these peptide−water simulations, we considered a coarse-grained description for the initial configurations (in bulk water), where each of the six backbone dihedral angles was started in either an "α-like" state (with $\phi = -60°$ and $\psi = -45°$) or a "β-like" state (with $\phi = -135°$ and $\psi = 135°$); e.g., initial configurations were started in the αααααα state, the ββββββ state, and mixtures of the two, but were not restricted to these states during the course of the simulations. In this way, we were able to access peptide configurations (e.g., arising from conformational transitions due to stiff torsions) that would not otherwise have been accessible in the time scale of our simulations. This also allowed us to locate candidate dihedral states where either the Lys−Asp or Arg−Asp side chains were presented on the same side of the peptide chain. Overall, we performed 10 production simulations of the peptide in bulk water, of duration ranging from 2 to 10 ns. The resulting viable configurations from these production runs were then transferred into the aqueous peptide−titania simulation cell, placed near the interface, and equilibrated as outlined above. This variety of approaches for generation of the initial configurations yielded a set of 24 production runs of the aqueous peptide−surface system, each of duration 1−2 ns.

In terms of structural analysis, all residue−surface vertical separation data presented herein were calculated from a baseline (in the direction perpendicular to the surface plane) of the five-coordinated Ti atoms on the titania surface. For Lys we measured from the surface to the terminal N atom, for Asp we measured from the surface to the carboxylate C atom, and for Arg we measured from the surface to the central C atom in the guanidinium group.

RESULTS

Effect of Interfacial Water Structuring. For all simulations of bound configurations, we found that interfacial binding occurred via a pair of oppositely charged species comprising either the Lys−Asp or Arg−Asp groups (referred to herein as KD and RD, respectively) regardless of the initial configurations used. These KD and RD configurations appeared to bind at the interface via the first two layers of water and are denoted as "indirect" geometries, typically, but not always (vide infra) remaining attached at this structured water bilayer for over 2 ns of the production run. Parts a and b of Figure 1 show an example of the resulting vertical and lateral water density profiles of a typical aqueous peptide−titania interface, for an indirect RD configuration, clearly indicating that the Asp and Arg groups do not perturb the first or second water layers. Figure 1c shows representative snapshots of the KD and RD indirect configurations, revealing the Asp carboxylate to bind via the H atoms presented outward from the surface because of the average orientation of the first layer of water. The Arg/Lys groups bind via the O atoms presented outward (on average) in the second water layer. This orientational ordering of water at the aqueous titania interface has been noted in previous simulations (47, 48). Similar to the experimental findings for peptide−DNA binding (42), our simulations suggest that the initial stages of recognition at the hydrophilic titania surface occur via the peptide binding to structured water at the interface.

The abundance of charged moieties in this sequence and the flexibility of the Lys and Arg side chains provide ample opportunities for electrostatically driven binding (21), via these orientationally structured water layers. The variety of binding configurations that we have identified in our simulations add further weight to our proposal from previous work that strong-binder sequences are those that confer a range of possible strong-binding conformations (35). Although we generated many different initial geometries for our peptide−surface simulations, we believe our KD and RD configura-

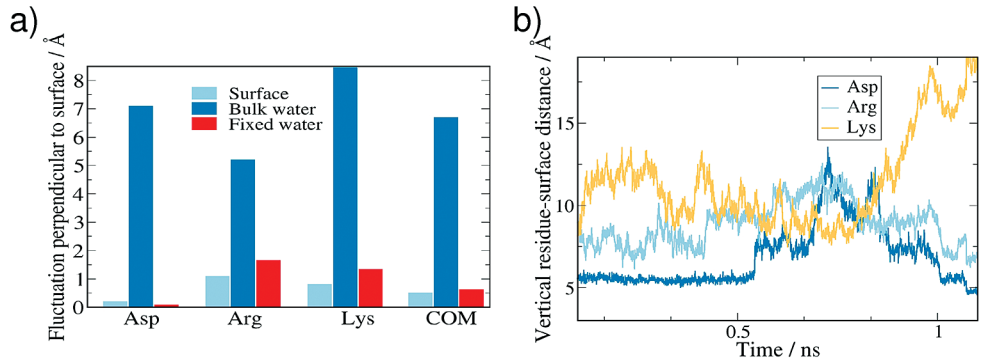

FIGURE 2. (a) Trajectory-averaged fluctuations of the vertical surface−residue distance for a typical binding configuration ("Surface"). "Fixed water" indicates binding via a fixed water bilayer with the titania slab removed from the simulation cell. "Bulk water" shows the average fluctuations in a bulk solution (no surface present). "COM" indicates the fluctuation in the distance from the surface to the center of mass of the peptide. (b) Typical profiles of the surface−residue distance for a remodeling event.

tions to be quite general; in contrast, it is possible to match the periodicity of the backbone carbonyls (in an extended peptide) onto the periodicity of the undercoordinated surface Ti atoms to contrive a "direct" multisite configuration. While such a configuration has been tested and shown to bind to the surface in our simulations, this mode is entirely dependent on the periodicity of the rutile (110) surface and is not an appropriate binding model for disordered titania surfaces. Our two-site binding configurations, whether directly or indirectly attached, do not depend on the presentation of specific lateral periodicity in the underlying inorganic material.

Most of our KD and RD configurations bound via the first two water layers showed reasonable stability (remaining bound over 2 ns of production simulation) yet also showed flexibility on occasion. We gauged the stability of the peptide at the interface by calculating the root-mean-squared deviation in the side chain−surface vertical distance over our production runs for KD and RD indirect bound configurations. These fluctuations, for a KD configuration, are shown as light-blue bars in Figure 2a. For comparison, the same vertical fluctuations were calculated for these configurations without the presence of the titania surface (e.g., in bulk water), shown as dark-blue bars in Figure 2a. By this, we mean that we calculated fluctuations for the peptide along the *z* axis of the periodic simulation cell (the choice of the other principal axes did not significantly change the trends of these fluctuations). We also ran simulations of these typical RD and KD indirect configurations where the titania slab was removed, and the first two layers of water were held fixed in space, with all other molecules allowed freedom to move, shown (for the same KD configuration) as red bars in Figure 2a. A similar set of data is presented for a typical RD configuration in Figure S1 of the Supporting Information. These data underscore the significance of the interaction with the structured water layers rather than with the titania itself because the degree of (considerable) peptide stability between simulations with both "frozen" and "free" water layers is comparable, while the peptide alone (in bulk water with no surface present) possesses significant freedom to move. In other words, the lack of fluctuations of the peptide when adsorbed at the interface is not due to any inherent stiffness in the peptide.

However, we suggest that the interplay between the interfacial stability and intrapeptide flexibility is key for strong-binding peptides; we attribute the properties of strong-binder sequences, in part, to the ease with which the peptide geometry may remodel its geometry at the interface. That is, ideally the initial binding of the charged groups at the interface should not be so strong that the peptide backbone becomes locked into a strained geometry upon contact at the interface. By way of comparison, X-ray crystallographic studies of ferritin−hexapeptide conjugates (57) also suggest a degree of mobility for this hexapeptide. Figure 2b shows a profile of the side chain−surface distance illustrating a typical remodeling event for an indirect RD configuration, taking place over a 1 ns subinterval in a typical production simulation. In this case, Arg detaches from the surface while at the same time the Lys group attaches onto the surface, only for this geometry to revert back to the RD configuration. We suggest that these remodeling events may be beneficial in the case where the eventual ingress of a peptide/protein at the interface will cause displacement of the structured waters in the first and second layers, resulting in direct surface contact in a favorable preconfigured geometry.

Effect of Alanine Mutations. While the RD and KD indirect configurations mostly exhibited pronounced stability at the water bilayer interface, some of the alanine mutants of RKLPDA exhibited significantly less stability. In all cases, we performed alanine mutations by taking the resulting stable wild-type binding configuration from the production simulation, mutating the residue in question to alanine, equilibrating (following the same procedure as that outlined in the Methods section), and following with a production run, using the same conditions as those outlined in the Methods section. The Asp−water interaction appears to be vital to indirect binding; mutation of Asp for Ala (RKLPAA) in either the KD or RD indirect configuration led to the expected result of detachment from the titania−water interface within 2 ns of production simulation (an example is shown in Figure S2 of the Supporting Information). However, mutation of Pro and Lys yielded behaviors unexpected from a purely electrostatically-driven binding hypothesis. Mutation of the neutral Pro for Ala (RKLADA) in our indirect configurations led to either partial or total detach-

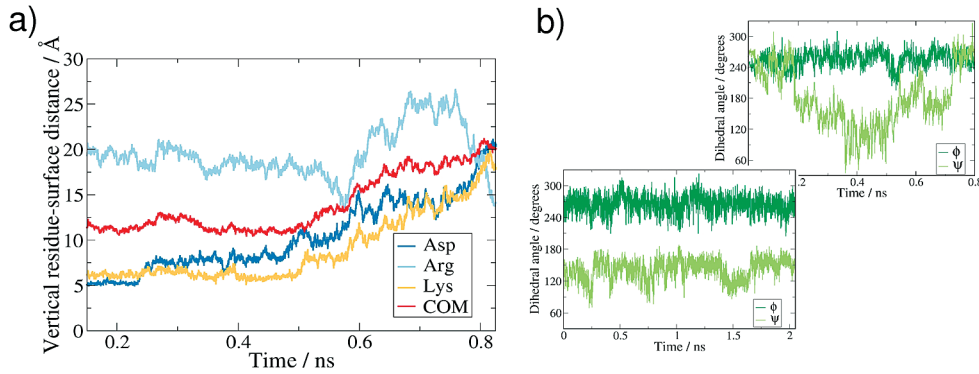

FIGURE 3. (a) Typical profiles of the surface−residue distance for the Pro mutant RKLADA, showing detachment from the surface. "COM" indicates the distance from the surface to the center of mass of the peptide. (b) Typical values of the backbone dihedral angles (ϕ and ψ) in the center of the peptide for the wild-type (front) and Pro (back) mutant.

ment of the peptide from the interface, confirmed by profiles of the vertical distance of each residue from the surface as a function of time, shown in Figure 3a for a typical total detachment event of a KD configuration (see Figure S3 of the Supporting Information for a profile yielding partial detachment of an RD configuration). Because Pro is well-known to confer structural rigidity, we suspected that the detachment mechanism of this mutant sequence was due to increased flexibility of the backbone. This was confirmed in Figure 3b by the contrast in profiles of the backbone dihedral angles (ϕ and ψ) as a function of time, for the same KD mutant trajectory as that shown in Figure 3a, at position 3 in the sequence (around Leu) for the wild-type and Pro mutant (see Figure S4 of the Supporting Information for data around position 4 for both sequences). These enhanced fluctuations in the dihedral angle at positions 3 and 4 in RKLADA confer relatively greater lability at the interface compared with the wild-type, and consequently we propose that these fluctuations could result in a lower binding affinity (given the noted total and partial detachment events). Further, our simulations of RKLPDA and RKLADA at the interface indicate that RKLADA favors the formation of relatively more compact configurations (Figures S5 and S6 of the Supporting Information). It is conceivable that sequences that favor more compact structures in a bulk solution may, in general, exhibit lower binding affinities than sequences that favor extended conformations, depending on the strength of the interaction between the peptide and surface (58).

Finally, we offer an explanation for the anomalous behavior of the Lys mutant, RALPDA, where mutation was observed to *not* diminish the binding affinity (21). From the viewpoint of a purely electrostatically driven binding hypothesis, one might naively expect mutation of Lys to yield a decrease in the binding affinity. In investigating this, we originally noted a small number of occasions where the wild-type, in both RD and KD indirect configurations, would detach from the water layers. In our analysis of these detachment events, we noticed a common feature, notably the approach and close contact between the Lys ammonium and the Asp carboxylate (and adjacent backbone carbonyl). We propose that this close, intrapeptide Lys−Asp interaction competes to the detriment of the water−Asp and water−Lys contacts for a KD configuration (and similarly competes with the water−Asp contact for an RD configuration). A typical snapshot of a KD configuration just prior to detachment via this mechanism is shown in Figure 4a. For this trajectory, the vertical distance profiles with time are shown in Figure 4b for the Asp/Arg/Lys groups, alongside the Lys−Asp and Lys−carbonyl distances for the same trajectory, indicating the time correlation of close Lys−Asp contact with the detachment event. Clearly, the Lys mutant RALPDA cannot support this competitive intrapeptide interaction, preventing this detachment mechanism from occurring. It is in this sense that we propose that the Lys mutant sequence may have more stability at the interface than the wild-type sequence, suggestive of a concomitant increase in the binding affinity for the Lys mutant, as noted in the alanine scan experiments (21). In Figure 4c, typical residue−surface distance profiles are shown, this time for an RD configuration, for the wild-type (which detaches from the surface by around 0.75 ns) and the corresponding Lys mutant, underscoring the stability of the mutant over the duration of the production simulation. The corresponding stable binding configuration of the Lys mutant, RALPDA, is shown in Figure 4d. The Lys−Asp contact for this RD configuration was again featured in the wild-type trajectory (Figure S7 of the Supporting Information).

DISCUSSION

The results presented herein are intended to form a foundation for further studies, with our immediate focus being the initial encounter between the peptide and the interfacial environment of the titania−water interface. While we recognize that our simulations only probe the initial stages of binding at the peptide−titania interface, our findings also suggest possible consequences that may take place after the initial contact is made, particularly in the migration of the charged groups from "indirect" to "direct" surface contact. We did not explore the possible mechanisms for this migration, but we did perform simulations of analogous "direct" KD and RD configurations for comparison. In these simulations, we took an existing, stable KD configuration and simply moved the peptide (in this conformation) into direct contact with the surface, before carefully resuming the simulation. The peptide conformation changed very little in

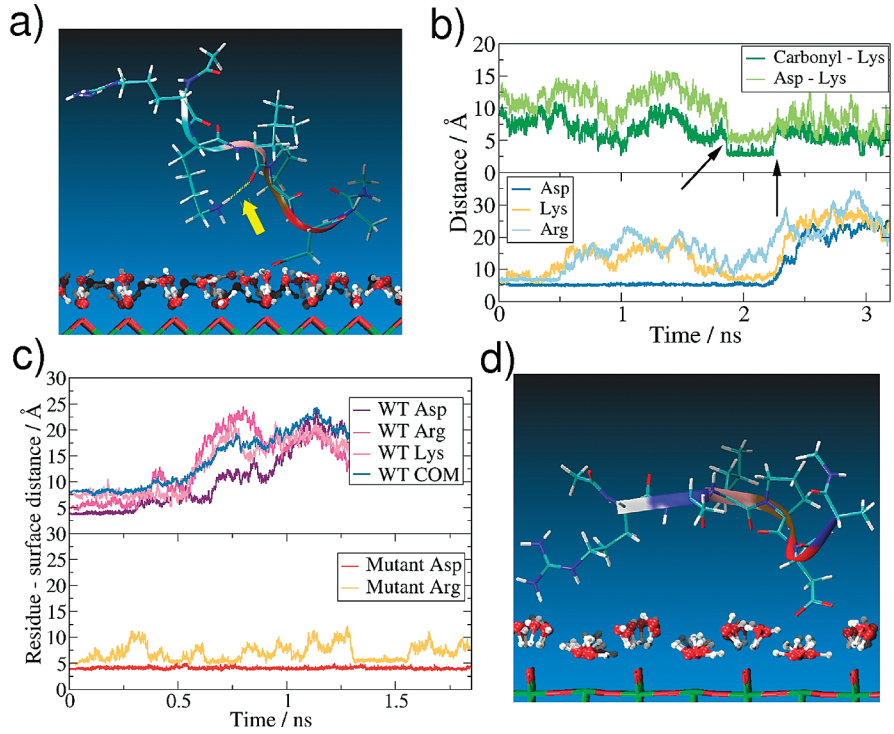

FIGURE 4. (a) Snapshot of the wild-type prior to detachment, with the Lys−carbonyl contact as indicated. (b) Bottom: corresponding surface−residue distance profiles for a typical detachment event of the wild-type. Top: corresponding Lys−carbonyl and Lys−Asp distances. The arrows indicate the onset of close correlated contact and the time of detachment, respectively. (c) Top: distance profiles for the wild-type in an RD configuration, prior to an intrapeptide-mediated detachment event. Bottom: distance profiles for the corresponding Lys mutant RALPDA, showing pronounced stability compared with the wild-type. (d) Snapshot of a stable Lys mutant RD configuration.

this process. We found that the total potential energy difference between the "direct" and "indirect" cases was very small (roughly 7 kcal mol^{-1}) in favor of the "direct" case. We performed a similar simulation for a stable RD configuration, and in this case, the total potential energy difference indicated that the "indirect" system was favored, this time by roughly 8 kcal mol^{-1}. We attribute these differences to the differences in the potential energy of the direct Asp−Ti and Arg/Lys−O interactions versus those for the water−Ti and water−O interactions because the peptide configuration (and, hence, the intrapeptide potential energy) did not change significantly in moving from "direct" to "indirect" contact. However, we place the error bars on these potential energy differences as being almost an order of magnitude larger than the differences themselves; as such, these results are inconclusive, and we cannot identify which mode of contact is more preferable on the basis of potential energy differences alone. This example has only probed the direct versus indirect differences for two particular configurations. However, because one strategy (of many) that we used in obtaining initial configurations was to use implicit solvent runs (which by definition will favor direct contact, vide infra), we did sample numerous direct-contact configurations in our explicit solvent runs. As outlined below (vide infra), many of these flat, direct-contact configurations did not remain flat on the surface once the interface was exposed to liquid water. One further point to add is that, if the surface is mostly hydroxylated, the issue of "direct" contact becomes rather academic. In our case, as was already outlined in the Methods section, the difference (in a structural sense) in the peptide "seeing" a nonhydroxylated surface via the first/second adsorbed water layers versus the peptide "seeing" a fully hydroxylated surface (where, therefore, the first/second water layers are now covalently attached) should not be great for the purposes of our study. We believe a more in-depth study of the balance between "direct" and "indirect" contact for this system should await the construction of a more detailed structural model of the surface (disordered titania, with a variation of hydroxylation state) and a strategy to sufficiently sample the peptide conformation under aqueous conditions, such that meaningful estimates of the entropy changes can be captured.

Despite being unable to gain meaningful calculated estimates of the entropy changes upon adsorption, we suggest that the profundity of this water structuring at the aqueous titania interface might lead to the thermodynamic favoring of direct attachment (via the peptide) when the peptide is attached to a much larger entity, e.g., the PIII coat of the M13 phage (21). Our argument is as follows. Previous experimental (59) and simulation studies (47, 48) both agree that the extent of water structuring does not persist further than 15 Å away from the titania surface. As seen in Figure 1a, at least four distinct structured water layers are apparent at the interface, with the first and second layers showing the most structuring. While, for example (in a peptide−phage system), we might assume the peptide itself could eventually disrupt the first and second water layers, we also propose that the larger entity (in this example the phage) may be brought sufficiently close to the surface that structured waters from layers 3 and 4 will be released back into the

bulk. Even in the idealized case where the long axis of the phage is oriented perpendicularly to the surface, one can estimate (based on the rough dimensions of the M13 phage) the release of hundreds of waters from layers 3 and 4. We also propose that the resulting entropic gain may exceed the peptide entropy lost due to direct attachment of the charged moieties at the surface, especially considering the additional mobility constraints imposed by the attachment of the peptide to the phage. Such an attachment process for the free (e.g., not phage-attached) peptide would not displace as many structured waters as a phage-attached peptide, so it is possible that the entropic gain is not as large in this latter case. This proposal is consistent with the measurements of Shiba and co-workers, who observed that the binding affinity of the free peptide (60) (not attached to a phage) was diminished relative to the phage-bound peptide. Shiba and co-workers attributed the greater binding affinity observed for the phage-bound peptide to the number of peptide chains displayed on each phage (61) (usually about five copies of the peptide per phage). In light of our findings, we suggest the reason, at least in part, could also be attributed to the entropic gain in binding free energy resulting from the phage (to which the peptide is attached), displacing and therefore releasing additional orientationally ordered water molecules in layers 3 and 4 from the interface and into the bulk. This proposed entropic effect may also play a part in rationalizing previous observations of reversible−irreversible binding transitions at the aqueous protein−titania interface (62), where again a large protein has a far greater potential for displacing a large number of structured waters in the more distant region of the interface, compared with a free peptide.

Some additional discussion of the water structuring at the aqueous titania interface is warranted. We have based our description of this interface on the model reported by Předota et al. (47), which combined a modified version of the Bandura potential for titania with the SPC/E model of water. The simulation results of Předota et al. were extensively validated in detail against X-ray studies (59), with excellent agreement found between these simulations and experiments, in particular with reference to the positions of the structured water layers. In a previous study (48), we reported simulations of the aqueous titania interface using a modified description of the force field used by Předota et al. (47), whereby we used a modified version of the TIP3P force field (51) to describe water instead of SPC/E; this is the description we used in this current work. The TIP3P model was chosen for reasons of harmonization with the CHARMM (50) force field used to describe the peptide. The simulation results from our previous work demonstrated excellent agreement with both the previous simulations of Předota et al. (despite the use of a different force field for water) and also the experimental X-ray studies. Nevertheless, while some of the gross features of this interfacial water structuring appear to have been recovered in our model, it would be interesting to probe more subtle effects via the use of more sophisticated water models (63) in the future.

In a similar vein, the reliability of the peptide−titania force field also warrants discussion. Unfortunately, unlike the case of the water−titania system, we do not have experimental structural data available for comparison. The determination of reliable cross-term contributions for surface−molecule interactions is necessary for describing the water−surface and peptide−surface contributions on an equal footing (64). In many cases, force fields describing inorganic materials are based on the Born model of solids and as such contain relatively large partial charges distributed over atomic sites, whereas biomolecule force fields such as CHARMM typically use partial charges of relatively smaller value. In such a case, straightforward application of the Lorentz−Berthelot mixing rules for nonbonded interactions gives problematic behavior (65, 66), because of this lack of harmonization between the electrostatic models describing the organic and inorganic components. However, in our case the titania component of our force field was designed with this harmonization in mind, and the partial charges on the titania have been constructed to fall in line with the partial charges on water, via the O atoms present in both species (47, 67). In this sense, while we have made use of the Lorentz−Berthelot mixing rules for the peptide−titania interactions, we propose this to be appropriate given the origins of the titania force field used here. However, we also remain cautious concerning interpretation of the subtle energetic details of these interfacial systems.

Our proposed intrapeptide detachment mechanism is based on the ability of the Lys and Asp side chains to form stable intramolecular interactions (based on the ammonium hydrogen bonding to the backbone carbonyl, in addition to the electrostatic interaction between the ammonium and carboxylate). The relative positioning of these residues in the peptide sequence may facilitate this effect; from circular dichroism spectroscopy measurements, Marqusee and Baldwin (68) inferred the presence of stabilizing Lys−Glu ion pairs/salt bridges in alanine-based peptides, for sequences containing a spacing between Lys and Glu of four residues (signified by the notation $i + 4$). The role of $i + 4$ Lys−Glu ion pairing in the helix stability has also been noted in atomistic MD simulations (69), where, in addition to Lys−Glu salt bridges, Lys−backbone carbonyl interactions were noted to also play a supporting role in the formation of intermediate structures. However, these experimental findings characterize Lys−Glu interactions, not Lys−Asp interactions. Moreover, the relative spacing of the Lys and Asp groups in the wild-type hexapeptide sequence is $i + 3$, one residue shorter than has been noted for spacings of stable Lys−Glu pairings. We propose that the shorter $i + 3$ Lys−Asp spacing is stable in RKLPDA because the side chain of Asp is shorter than the side chain of Glu by one methylene spacer unit, such that the distance to be bridged by the two oppositely charged species is similar to that for $i + 4$ Lys−Glu intrapeptide interactions. Further evidence for intrapeptide Lys−Asp salt-bridge contacts has been reported in atomistic simulations of amyloid β-protein monomers, where the salt bridges

were found to stabilize the monomer configuration (70). Interestingly, we did not find any evidence of Arg−Asp intrapeptide interactions for any of the surface-bound configurations, despite these residues possessing an $i + 4$ spacing in the sequence. However, our own MD studies of the wild-type peptide in a bulk solution (data not shown) revealed that while an Arg−carbonyl intrapeptide contact could be formed, it appeared less stable (remaining in contact for less than 1.5 ns on average) compared with the Lys−Asp and Lys−carbonyl intrapeptide contacts (typically remaining in contact for 5−7 ns). This diminished stability might be due to the relative positions of Arg and Asp; to test this, further simulations could be run with the positions of the Arg and Lys residues swapped. This may also be due to an inherently weaker interaction between Asp and Arg perhaps because of the more bulky nature of the guanidinium group. We propose that the formation of intrapeptide interactions involving residues that interact with the surface may, in general, provide competition that could be detrimental to the formation of a stable contact at the interface. Eliminating sources of such self-interaction may be key to obtaining a reliable and predictable stability at the peptide−inorganic interface.

We note that, in the context of the point mutations, the experimental data (quartz crystal microbalance and dissipation measurements) that we used for comparison are inferred to connect directly with the relative binding affinity of the peptides at the interface (21). In addition, the actual binding constants for the free and phage-attached wild-type peptides have also been reported (60). However, in order to estimate the binding constants from simulation, we need to calculate either the ratio of the adsorption/desorption rate constants or the change in the free energy of adsorption of the peptide at the surface. Unfortunately, the degree of statistical sampling required to obtain meaningful free energies of binding *in aqueous solution* puts such calculations out of reach for these systems at present. The results presented in this work are intended to form a foundation for further studies, with our immediate focus being the initial encounter between the peptide and the interfacial environment of the titania−water interface. The issue of free-energy calculations notwithstanding, on the basis of exploring the potential energy landscape alone, we recognize that our simulations reported here are not the result of exhaustive conformational sampling. Inherent to resolving this sampling problem is the need (or not) for an explicit description of the solvent. While examples of more sophisticated sampling protocols have been demonstrated recently in modeling the protein−hydroxyapatite interface (71, 72), the effectiveness of such an approach appears to hinge, at least in part, on the necessity of using an implicit solvent in describing the interactions at the interface. Neglect of an explicit solvent may be appropriate in some cases, as was recently explored for peptide−nanotube interfaces (73); however, we are not convinced that neglect of explicit solvation at the peptide−titania interface is appropriate, given the degree of water structuring involved (as was reinforced by experimental studies (59)). Because we ran some initial simulations in the presence of an implicit solvent (one of the many strategies that we used to obtain initial configurations for our simulations), we are in a position to comment further on this issue. All of the resulting configurations from our implicit-solvent peptide−titania runs were very flat, such that the contact between the peptide and surface was maximized with the backbone carbonyl groups positioned close to the surface sites. However, upon the addition of explicit water to our simulation cell, followed by careful equilibration (as detailed in the Methods section), we noted that in an overwhelming majority of cases the center of the peptide chain gradually moved away from the surface, giving the 3D shapes shown in Figure 1c. In summary, the configurations from our implicit-solvent runs were on the whole very different from explicit-solvent simulations. Further, we tried using a couple of implicit-solvent models, with widely differing results; the ASP (55, 56) model employed here yielded extended conformations on the surface, while the generalized-Born solvation model (74) gave globular conformations making little surface contact. It would seem that, if implicit solvation is to be used in modeling such *aqueous* peptide−inorganic interfaces, systematic comparative studies of adsorbate behavior in both implicit and explicit solvents will be needed for these interfaces to assess the reliability of this approach (75). We add that the importance of accounting for water structuring when modeling interfacial adsorption processes is not confined to titania surfaces, having recently also been highlighted for calcite and magnesite surfaces (76) and quartz surfaces (41). Nevertheless, despite the lack of exhaustive sampling in our system, in part hampered by the use of an explicit solvent, our simulation results, while not providing an immediate measure of the equilibrium binding affinity, show behavior that could be interpreted as indicative. As a further caveat, we also point out that our simulations of this peptide have only described the trans form of Pro. The likelihood of finding the cis form in the imide bond preceding the Pro in unstructured peptides is nonzero and may be as great as 30% (77, 78), depending on the local sequence around the Pro residue. Further, Sano and Shiba suggested a possible structural role of *cis*-Pro in the binding of this hexapeptide at the titania surface (21). While our studies here indicate that Pro can play a structural role in the trans form, we recognize that a more complete account of the initial peptide−titania binding should account for this fact and plan to address this in future studies.

The role of flexibility in the binding of peptides at the aqueous inorganic interface is one that we propose is not necessarily straightforward. In particular, in our Results section, we suggest that a *balance* between the intrapeptide flexibility and interfacial stability will be important. By this, we mean the following. We propose some degree of flexibility to be beneficial in the sense that such a peptide may presumably access a greater number of stable binding configurations compared with a peptide that is not as flexible. However, it is conceivable that a peptide with *excessive* flexibility may feature low-energy barriers to de-

forming out of the conformation needed for it to bind at the interface. We propose that the balance lies in the flexibility of the peptide and the strength of the interaction between the peptide and surface interface; the peptide should be flexible enough to be able to find a good binding configuration, yet once this stable binding configuration is established, the peptide should have sufficient intrapeptide stability in order to maintain this binding configuration. Furthermore, the notion of *localized* stiffness/flexibility in the peptide chain may be more meaningful in this context; e.g., the position of Pro in the center of the chain gives rise to a peptide that has flexible ends (possibly good for initially finding a stable binding configuration) with a stiff center (perhaps useful in maintaining this binding configuration). This hypothesis could be probed with simulations where the sequence of the peptide is scrambled; e.g., we could move Pro to one of the chain ends, say with the sequence RKLADP. Such simulations are planned as future work in this area (vide infra).

While in this work MD simulations have been used to infer connections with experimental data relating to point mutations, the next step is to go beyond this, e.g., to simulate *scrambled* strong-binder sequences. This approach would present new opportunities for simulation to connect with the underexplored area of peptide *specificity* (19, 79). Understanding how to manipulate the preferential adsorption of peptides will be fundamental to the successful exploitation of these interfaces in the environmentally friendly fabrication of nanostructured materials in an aqueous solution.

CONCLUSIONS

Atomistic MD simulations have been used to model the initial stages of the adsorption of an experimentally identified hexapeptide sequence at the aqueous titania interface. Our simulations suggested that there may be at least four layers of structured water at the interface, with the most significant being the first two layers, via which the hexapeptide interacts with the titania surface. Two-point interfacial contact was a recurring theme of our simulations, typically via a pair of oppositely charged moieties (the aspartate teamed with either the ammonium or guanidinium groups), that interacted with different layers of the orientationally structured water at the interface. Our simulations of alanine point mutants indicated that, as suggested in the existing alanine scan experimental data, the presence of a charged Asp group was vital for maintaining peptide contact at the interface. Our results also suggest that mutation of the neutral Pro residue could lead to peptide detachment, again in line with the experimental observations, with the mechanism for detachment appearing to be due to an increase in the flexibility of the peptide backbone. Conversely, and as has been noted in the experiment, mutation of the charged Lys residue indicated a potentially greater stability of binding at the interface compared with that of the wild-type sequence because the Lys mutant could not access a detachment mechanism noted in the wild-type. This detachment mechanism was proposed to be facilitated by detrimental intrapeptide contact between the flexible Lys side chain and the Asp residue.

Acknowledgment. We gratefully acknowledge the computing resources of the Centre for Scientific Computing, University of Warwick, and the National Grid Service, U.K. This project was funded by the EPSRC Materials Modelling Consortium (Grant GR/S80127/01) "Modelling the Biological Interface with Materials".

Note Added after ASAP Publication. This article was released ASAP on June 10, 2009, with reference numbers incorrectly cited in the text. The correct version was posted on June 12, 2009.

Supporting Information Available: Vertical fluctuation comparisons for an RD configuration; surface−residue distance profiles for detachment of the Asp mutant; surface−residue distance profiles for partial detachment of the Pro mutant; dihedral angle fluctuations around position 4 for wild-type and Pro mutant; evidence of more compact structures for the Pro mutant; snapshot of the Lys−carbonyl intrapeptide contact in an RD configuration prior to detachment. This material is available free of charge via the Internet at http://pubs.acs.org.

REFERENCES AND NOTES

(1) Brown, S. *Nat. Biotechnol.* **1997**, *15*, 269.
(2) Whaley, S. R.; English, D. S.; Hu, E. L.; Barbara, P. R.; Belcher, A. M. *Nature* **2000**, *405*, 665.
(3) Sarikaya, M.; Tamerler, C.; Jen, A. K. Y.; Schulten, K.; Baneyx, F. *Nat. Mater.* **2003**, *2*, 577.
(4) Gray, J. J. *Curr. Opin. Struct. Biol.* **2004**, *14*, 110.
(5) Kriplani, Y.; Kay, B. K. *Curr. Opin. Biotechnol.* **2005**, *16*, 470.
(6) Tamerler, C.; Sarikaya, M. *Acta Biomater.* **2007**, *3*, 289.
(7) Baneyx, F.; Schwartz, D. T. *Curr. Opin. Biotechnol.* **2007**, *18*, 312.
(8) Dai, H. X.; Choe, W. S.; Thai, C. K.; Sarikaya, M.; Traxler, B. A.; Baneyx, F.; Schwartz, D. T. *J. Am. Chem. Soc.* **2005**, *127*, 15637.
(9) Peelle, B. R.; Krauland, E. M.; Wittrup, K. D.; Belcher, A. M. *Acta Biomater.* **2005**, *1*, 145.
(10) Zin, M. T.; Munro, A. M.; Gungormus, M.; Wong, N. Y.; Ma, H.; Tamerler, C.; Ginger, D. S.; Sarikaya, M.; Jen, A. K. Y. *J. Mater. Chem.* **2007**, *17*, 866.
(11) Nam, K. T.; Kim, D. W.; Yoo, P. J.; Chang, C. Y.; Meethong, N.; Hammond, P. T.; Chiang, Y. M.; Belcher, A. M. *Science* **2006**, *312*, 885.
(12) Tamerler, C.; Kacar, T.; Sahin, D.; Fong, H.; Sarikaya, M. *Mater. Sci. Eng., C* **2007**, *27*, 558.
(13) Krauland, E. M.; Peelle, B. R.; Wittrup, K. D.; Belcher, A. M. *Biotechnol. Bioeng.* **2007**, *97*, 1009.
(14) Meyers, S. R.; Hamilton, P. T.; Walsh, E. B.; Kenan, D. J.; Grinstaff, M. W. *Adv. Mater.* **2007**, *19*, 2492.
(15) Hattori, T.; Umetsu, M.; Nakanishi, T.; Tsumoto, K.; Ohara, S.; Abe, H.; Naito, M.; Asano, R.; Adschiri, T.; Kumagai, I. *Biochem. Biophys. Res. Commun.* **2008**, *365*, 751.
(16) Sano, K. I.; Yoshii, S.; Yamashita, I.; Shiba, K. *Nano Lett.* **2007**, *7*, 3200.
(17) Sengupta, A.; Thai, C. K.; Sastry, M. R. S.; Matthaei, J. F.; Schwarz, D. T.; Davis, E. J.; Baneyx, F. *Langmuir* **2008**, *24*, 2000.
(18) Oren, E. E.; Tamerler, C.; Sahin, D.; Hnilova, M.; Seker, U. O. S.; Sarikaya, M.; Samudrala, R. *Bioinformatics* **2007**, *23*, 2816.
(19) Goede, K.; Busch, P.; Grundmann, M. *Nano Lett.* **2004**, *4*, 2115.
(20) Hnilova, M.; Oren, E. E.; Seker, U. O. S.; Wilson, B. R.; Collino, S.; Evans, J. S.; Tamerler, C.; Sarikaya, M. *Langmuir* **2008**, *24*, 12440.
(21) Sano, K. I.; Shiba, K. *J. Am. Chem. Soc.* **2003**, *125*, 14234.
(22) Hayashi, T.; Sano, K. I.; Shiba, K.; Kumashiro, Y.; Iwahori, K.; Yamashita, I.; Hara, M. *Nano Lett.* **2006**, *6*, 515.
(23) Kashiwagi, K.; Tsuji, T.; Shiba, K. *Biomaterials* **2009**, *30*, 1166.
(24) Kokubun, K.; Kashiwagi, K.; Yoshinari, M.; Inoue, T.; Shiba, K. *Biomacromolecules* **2008**, *9*, 3098.

(25) Goobes, G.; Goobes, R.; Scheuler-Furman, O.; Baker, D.; Stayton, P. S.; Drobny, G. P. *Proc. Natl. Acad. Sci. U.S.A.* **2006**, *103*, 16083.
(26) Chen, P. H.; Mou, Y. H.; Tsai, Y. L.; Guo, S. M.; Huang, S. J.; Chan, J. C. C. *J. Am. Chem. Soc.* **2008**, *130*, 2862.
(27) Delak, K.; Collino, S.; Evans, J. S. *Langmuir* **2007**, *23*, 11951.
(28) Peelle, B. R.; Krauland, E. M.; Wittrup, K. D.; Belcher, A. M. *Langmuir* **2005**, *21*, 6929.
(29) Seker, U. O. S.; Wilson, B.; Dincer, S.; Kim, I. W.; Oren, E. E.; Evans, J. S.; Tamerler, C.; Sarikaya, M. *Langmuir* **2007**, *23*, 7895.
(30) Evans, J. S.; Samudrala, R.; Walsh, T. R.; Oren, E. E.; Tamerler, C. *MRS Bull.* **2008**, *33*, 514.
(31) Braun, R.; Sarikaya, M.; Schulten, K. *J. Biomater. Sci., Polym. Ed.* **2002**, *13*, 747.
(32) Oren, E. E.; Tamerler, C.; Sarikaya, M. *Nano Lett.* **2005**, *5*, 415.
(33) Kantarci, N.; Tamerler, C.; Sarikaya, M.; Haliloglu, T.; Doruker, P. *Polymer* **2005**, *46*, 4307.
(34) Thai, C. K.; Dai, H. X.; Sastry, M. S. R.; Sarikaya, M.; Schwartz, D. T.; Baneyx, F. *Biotechnol. Bioeng.* **2004**, *87*, 129.
(35) Tomásio, S. D.; Walsh, T. R. *Mol. Phys.* **2007**, *105*, 221.
(36) Wang, S.; Humphreys, E. S.; Chung, S.-Y.; Delduco, D. F.; Lustig, S. R.; Wang, H.; Parker, K. N.; Rizzo, N. W.; Subramoney, S.; Chiang, Y.-M.; Jagota, A. *Nat. Mater.* **2003**, *2*, 196.
(37) Caravetta, V.; Monti, S. *J. Phys. Chem. B* **2006**, *110*, 6160.
(38) Monti, S. *J. Phys. Chem. C* **2007**, *111*, 6086.
(39) Schravendijk, P.; Ghiringhelli, L. M.; Delle Site, L.; van der Vegt, N. F. A. *J. Phys. Chem. C* **2007**, *111*, 2631.
(40) Ghiringhelli, L. M.; Hess, B.; van der Vegt, N. F. A.; Delle Site, L. *J. Am. Chem. Soc.* **2008**, *130*, 13460.
(41) Notman, R.; Walsh, T. R. *Langmuir* **2009**, *25*, 1638.
(42) Shakked, Z.; Guzikevich-Guerstein, G.; Frolow, F.; Rabinovitch, D.; Joachimiak, A.; Sigler, P. B. *Nature* **1994**, *368*, 469.
(43) Healy, K. E.; Ducheyne, P. *Biomaterials* **1992**, *13*, 553.
(44) Lausmaa, J.; Kasemo, B.; Mattson, H. *Appl. Surf. Sci.* **1990**, *44*, 133.
(45) Roddick-Lanzilotta, A. D.; Connor, P. A.; McQuillan, A. J. *Langmuir* **1998**, *14*, 6479.
(46) Roddick-Lanzilotta, A. D.; McQuillan, A. J. *J. Colloid Interface Sci.* **2000**, *227*, 48.
(47) Předota, M.; Bandura, A. V.; Cummings, P. T.; Kubicki, J. D.; Wesolowski, D. J.; Chialvo, A. A.; Machesky, M. L. *J. Phys. Chem. B* **2004**, *108*, 12049.
(48) Skelton, A. A.; Walsh, T. R. *Mol. Simul.* **2007**, *33*, 379.
(49) Smith, W.; Forester, T. R. *J. Mol. Graphics* **1996**, *14*, 136.
(50) MacKerell, A. D.; Bashford, D.; Bellott, M.; Dunbrack, R. L.; Evanseck, J. D.; Field, M. J.; Fischer, S.; Gao, J.; Guo, H.; Ha, S.; Joseph-McCarthy, D.; Kuchnir, L.; Kuczera, K.; Lau, F. T. K.; Mattos, C.; Michnick, S.; Ngo, T.; Nguyen, D. T.; Prodhom, B.; Reiher, W. E.; Roux, B.; Schlenkrich, M.; Smith, J. C.; Stote, R.; Straub, J.; Watanabe, M.; Wiorkiewicz-Kuczera, J.; Yin, D.; Karplus, M. *J. Phys. Chem. B* **1998**, *102*, 3586.
(51) Mark, P.; Nilsson, L. *J. Phys. Chem. A* **2001**, *105*, 9954.
(52) Nosé, S. *J. Chem. Phys.* **1984**, *81*, 511.
(53) Nosé, S. *Mol. Phys.* **1984**, *52*, 255.
(54) Hoover, W. G. *Phys. Rev. A* **1985**, *31*, 1695.
(55) Eisenberg, D.; McLachlan, A. D. *Nature* **1986**, *319*, 199.
(56) Wesson, L.; Eisenberg, D. *Protein Sci.* **1992**, *1*, 227.
(57) Yamashita, I.; Kirimura, H.; Okuda, M.; Nishio, K.; Sano, K. I.; Shiba, K.; Hayashi, T.; Hara, M.; Mishima, Y. *Small* **2006**, *2*, 1148.
(58) Mijajlovic, M.; Biggs, M. J. *J. Phys. Chem. C* **2007**, *111*, 15839.
(59) Zhang, Z.; Fenter, P.; Cheng, L.; Sturchio, N. C.; Bedzyk, M. J.; Předota, M.; Bandura, A.; Kubicki, J.; Lvov, S. N.; Cummings, P. T.; Chialvo, A. A.; Ridley, M. K.; Bénézeth, P.; Anovitz, L.; Palmer, D. A.; Machesky, M. L.; Wesolowski, D. J. *Langmuir* **2004**, *20*, 4954.
(60) Sano, K. I.; Sasaki, H.; Shiba, K. *Langmuir* **2005**, *21*, 3090.
(61) Sano, K. I.; Ajima, K.; Iwahori, K.; Yudasaka, M.; Iijima, S.; Yamashita, I.; Shiba, K. *Small* **2005**, *1*, 826.
(62) Ball, V.; Bentaleb, A.; Hemmerle, J.; Voegel, J.-C.; Schaaf, P. *Langmuir* **1996**, *12*, 1614.
(63) Ren, P.; Ponder, J. W. *J. Comput. Chem.* **2002**, *23*, 1497.
(64) Freeman, C. L.; Harding, J. H.; Cooke, D. J.; Elliott, J. A.; Lardge, J. S.; Duffy, D. M. *J. Phys. Chem. C* **2007**, *111*, 11943.
(65) Duffy, D. M.; Harding, J. H. *Langmuir* **2004**, *20*, 7630.
(66) Cormack, A. N.; Lewis, R. J.; Goldstein, A. H. *J. Phys. Chem. B* **2004**, *108*, 20408.
(67) Bandura, A. V.; Kubicki, J. D. *J. Phys. Chem. B* **2003**, *107*, 11072.
(68) Marqusee, S.; Baldwin, R. L. *Proc. Natl. Acad. Sci. U.S.A.* **1987**, *84*, 8898.
(69) Wang, W. Z.; Lin, T.; Sun, Y. C. *J. Phys. Chem. B* **2007**, *111*, 3508.
(70) Tarus, B.; Straub, J. E.; Thirumalai, D. *J. Am. Chem. Soc.* **2006**, *128*, 16159.
(71) Makrodimitris, K.; Masica, D. L.; Kim, E. T.; Gray, J. J. *J. Am. Chem. Soc.* **2007**, *129*, 13713.
(72) Masica, D. L.; Gray, J. J. *Biophys. J.* **2009**, *96*, 3082.
(73) Tomasio, S. M.; Walsh, T. R. *J. Phys. Chem. C* **2009**, *113*, 8778.
(74) Qui, D.; Shenkin, P. S.; Hollinger, F. P.; Still, W. C. *J. Phys. Chem. A* **1997**, *101*, 3005.
(75) Sun, Y.; Latour, R. A. *J. Comp. Chem.* **2006**, *27*, 1908.
(76) Freeman, C. L.; Asteriadis, I.; Yang, M.; Harding, J. H. *J. Phys. Chem. C* **2009**, *113*, 3666.
(77) Brandts, J. F.; Halvorson, H. R.; Brennan, M. *Biochemistry* **1975**, *14*, 4953.
(78) Stewart, D. E.; Sarkar, A.; Wampler, J. E. *J. Mol. Biol.* **1990**, *214*, 253.
(79) Tamerler, C.; Duman, M.; Oren, E. E.; Gungormus, M.; Xiong, X.; Kacar, T.; Parviz, B. A.; Sarikaya, M. *Small* **2006**, *11*, 1372.

AM9001666